Residence Time Distribution of a Cylindrical Microreactor

Jyh-Ping Hsu* and Tzu-Hsuan Wei

Department of Chemical Engineering, National Taiwan University, Taipei, Taiwan 10617

Received: December 19, 2004; In Final Form: March 3, 2005

The residence time distribution for the flow of liquid reactants containing electrolytes in a cylindrical microreactor is derived under the conditions of constant surface potential and negligible end effects. The influences of the key parameters, including the thickness of the double layer, the strength of the applied electric field, and the magnitude of the applied pressure gradient, on the behavior of residence time distribution are discussed. The results obtained provide necessary information for the design and optimization of microreactors which involve liquid electrolyte reactants. The results of the numerical simulation reveal that a thin double layer, a strong applied electric field, and a greater applied pressure gradient lead to a faster fluid flow and, therefore, a short residence time. We show that if $\kappa a \leq 0.001$ the residence time distribution can be approximated by that for the case of a laminar flow, and if $\kappa a \geq 500$, the residence time distribution can be approximated by that for the case of a plug flow, with κ and a being the reciprocal Debye length and the radius of the microreactor, respectively.

Introduction

Following the development of microelectromechanical systems[1] in the semiconductor industry, microfabrication techniques[2] have advanced dramatically in the past decade. In recent years, its applications were extended successfully to the chemical and biomedical industries.[3] The so-called microreactor,[4] that is, a reactor whose linear size is on the order of 100 μm, has drawn the attention of researchers of various areas. In comparison with conventional reactors, microreactors have the following merits: the capability of providing a large surface area per unit volume, essentially no scale-up problems when extending from lab scale to production scale, considerably reduced time and cost in factory design, and higher efficiency.[5−9] Also, the risks in transportation and storage of toxic chemicals can be reduced, and on-line sensors and controllers can be integrated to terminate and replace malfunctioning reactors without influencing the operation of other reactors. The fast heat and mass transfer rates of a microreactor make it tolerant of temperatures and pressures that are considerably higher than those employed in conventional reactors.[10,11] Furthermore, because of the small linear size, the reaction mechanisms of the reactions conducted inside a microreactor can be different from those conducted in conventional reactors, and it is possible that reactions that do not occur in the latter might occur in the former.[12]

When the linear size of a reactor decreases to the micrometer range, in addition to the driving forces for the flow of reactants/products, such as pressure gradient, usually applied to a macroreactor, other types of driving forces may also be present. For example, if liquid reactants contain electrolytes, the charge on the wall of a microreactor may lead to electroosmotic flow inside. Depending upon the charge conditions, the electroosmotic flow can be in the same or the opposite direction as that of the applied pressure gradient. Apparently, the electroosmotic flow can play a significant role in the determination of the residence time and the degree of mixing of the reactants in a microreactor. Although electroosmotic flow has been studied extensively,[13−28] relevant information about its influence on the residence time of liquid reactants inside a microreactor is very limited. Knowledge about the residence time distribution[29−31] of reactants in a reactor is essential to its design and optimization.

In this study, the residence time distribution for a long cylindrical microreactor is derived. In addition to an applied pressure gradient, an external electric field is applied to drive the flow of reactants inside. The latter renders more flexible reaction conditions, because the flow field can be adjusted through control of the concentration of reactants and the charged conditions on the reactor wall. The influences of the key parameters, including the pressure gradient, the strength of the applied electric field, and the concentrations of the reactants, on the behavior of the residence time distribution are investigated.

Theory

Referring to Figure 1, we consider the steady flow of a 1:1 electrolyte solution through a cylindrical microreactor of diameter $2a$ and length L. For simplicity, we assume the end effects are negligible and the flow inside the microreactor is fully developed. The cylindrical coordinates are adopted with the origin located at the axis of the microreactor. Let r and z be the radial and the axial coordinates, respectively. The surface of the microreactor is positively charged with electrical potential ψ_s. An external electrical field $E_z = -(\partial\phi/\partial z)$ and a pressure gradient $P_z = -(\partial P/\partial z)$ are applied in the z-direction, with ϕ and P being the electrical potential and the pressure, respectively. Let ϵ and μ be the dielectric constant and the viscosity of the electrolyte solution, respectively. For the present case, counterions flow in the z-direction, and the velocity of the liquid phase U is a function of r only.

Electrical Field

The electrical potential ϕ comprises two components, namely, the electrical potential in the absence of the applied electrical

* To whom correspondence should be addressed. Fax: 886-2-23623040. E-mail: jphsu@ntu.edu.tw.

10.1021/jp044231u CCC: $30.25
Published on Web 03/30/2005

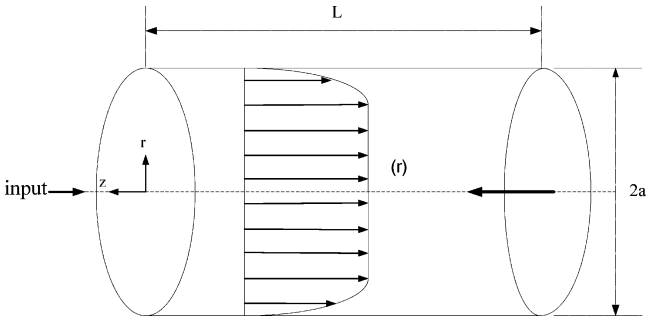

Figure 1. Schematic representation of the problem considered where the flow of liquid reactants containing electrolytes in a long cylindrical microreactor of length L, diameter $2a$, and surface potential ψ is driven by both a pressure gradient P_z and an electric field E_z in the z-direction; the cylindrical coordinates (r, θ, z) are adopted with the origin located at the axis of the microreactor, and $U(r)$ is the radial velocity distribution.

potential or the equilibrium potential $\psi(r)$ and that which arises from the applied electrical potential. We have

$$\phi = \phi(r, z) = \psi(r) - zE_z \tag{1}$$

The electrical potential is described by the Poisson equation. In cylindrical coordinates, we have

$$\frac{1}{r}\frac{\partial}{\partial r}\left(r\frac{\partial \phi}{\partial r}\right) + \frac{\partial^2 \phi}{\partial z^2} = -\frac{\rho_{el}}{\epsilon} \tag{2}$$

Equations 1 and 2 yield

$$\frac{1}{r}\frac{d}{dr}\left(r\frac{d\psi}{dr}\right) = -\frac{\rho_{el}}{\epsilon} \tag{3}$$

Suppose that the spatial distribution of the ionic species follows the Boltzmann distribution. Then, the number concentrations of cations n_+ and anions n_- can be described respectively by

$$n_+ = n_\infty \exp\left[\frac{F\psi}{RT}\right] \tag{4}$$

and

$$n_- = n_\infty \exp\left[\frac{F\psi}{RT}\right] \tag{5}$$

where n_∞ is the bulk number concentration of the electrolyte, and F and R are respectively the Faraday constant and the gas constant, and T is the absolute temperature. Therefore, ρ_{el} can be expressed as

$$\rho_{el} = F(n_+ - n_-) = Fn_\infty\left[\exp\left(-\frac{F\psi}{RT}\right) - \exp\left(\frac{F\psi}{RT}\right)\right] \tag{6}$$

If $F\psi/RT$ is sufficiently small, ρ_{el} can be approximated by

$$\rho_{el} = -2n_\infty \exp\left(\frac{F\psi}{RT}\right) \tag{7}$$

Substituting eq 7 into eq 3 yields

$$\frac{1}{r}\frac{d}{dr}\left(r\frac{d\psi}{dr}\right) = \kappa^2\psi \tag{8}$$

where $\kappa = (2IF^2/\epsilon RT)^{1/2}$ is the Debye−Huckel parameter, with I being the ionic strength. Suppose that the surface of the cylindrical wall remains at constant potential ψ_s. Then, the boundary conditions associated with eq 8 are

$$\psi = \psi_s, \quad r = a \tag{9}$$

$$\frac{d\psi}{dr} = 0, \quad r = 0 \tag{10}$$

The second condition arises from the symmetric nature of the present problem. Solving eq 8 subject to eqs 9 and 10 gives

$$\psi = \psi_s \frac{I_0(\kappa r)}{I_0(\kappa a)} \tag{11}$$

where I_0 is the zero-order modified Bessel function of the first kind.

Flow Field

Suppose that the electrolyte solution is a Newtonian fluid of constant physical properties. Also, the Reynolds number is small and the effect of gravity is unimportant. Under these conditions, the flow field can be described by

$$\mu\frac{1}{r}\frac{d}{dr}\left[r\frac{dU}{dr}\right] = \frac{dp}{dz} + \rho_{el}E_z \tag{12}$$

Substituting eq 11 into eq 7 gives

$$\rho_{el} = -\epsilon\kappa^2\psi_s\frac{I_0(\kappa r)}{I_0(\kappa a)} \tag{13}$$

Substituting eq 13 into eq 12, we obtain

$$\mu\frac{1}{r}\frac{d}{dr}\left[r\frac{dU}{dr}\right] = \frac{dp}{dz} - \epsilon\epsilon_0\psi_s\kappa^2E_z\frac{I_0(\kappa r)}{I_0(\kappa a)} \tag{14}$$

If the surface of the cylinder is no-slip, then the boundary conditions associated with eq 14 are

$$U = 0, \quad r = a \tag{15}$$

$$\frac{dU}{dr} = 0, \quad r = 0 \tag{16}$$

The second boundary condition arises from the symmetric nature of the present problem. Solving eq 14 subject to eqs 15 and 16 gives

$$U(r) = \frac{a^2}{4\mu}\frac{dp}{dz}\left[1 - \left(\frac{r}{a}\right)^2\right] - \frac{\epsilon\psi_s}{\mu}E_z\left[1 - \frac{I_0(\kappa r)}{I_0(\kappa a)}\right] \tag{17}$$

Residence Time Distribution (RTD)

Knowledge about the residence time distribution of a reactor is essential to the assessment of its performance. This distribution can be determined from the steady-state velocity distribution $U(r)$. For the case when pressure gradient is not applied, $P_z = 0$, eq 17 yields

$$t = \frac{L}{U(r)} = \frac{L}{A\left[1 - \frac{I_0(\kappa r)}{I_0(\kappa a)}\right]} \tag{18}$$

where $A = -\epsilon\psi_s E_z/\mu$. Differentiating eq 18 with respect to r, we obtain

$$dt = \frac{L\kappa}{AI_0(\kappa a)} \frac{I_1(\kappa r)\, dr}{\left[1 - \frac{I_0(\kappa r)}{I_0(\kappa a)}\right]^2} \tag{19}$$

The residence time distribution (RTD), $E(t)$, can be expressed as

$$E(t) = \frac{dV}{V_0}\frac{1}{dt} = \frac{U(r)2\pi r\, dr}{V_0}\frac{1}{dt} \tag{20}$$

Substituting eq 19 into eq 20 yields

$$E(t) = \frac{2\pi A^2 I_0(\kappa a)}{V_0 \kappa L} \frac{\left[1 - \frac{I_0(\kappa r)}{I_0(\kappa a)}\right]^3 r}{I_1(\kappa r)} \tag{21}$$

where I_1 is the first-order modified Bessel function of the first kind. The volumetric flow rate V_0 can be expressed as

$$V_0 = -\frac{\epsilon\psi_s}{\mu} A_c E_z \left[1 - \frac{2I_1(\kappa a)}{(\kappa a) I_0(\kappa a)}\right] \tag{22}$$

where A_c is the cross-sectional area of the cylinder.

If a pressure gradient P_z is applied, eq 17 leads to

$$t = \frac{L}{U(r)} = \frac{L}{B\left[1 - \left(\frac{r}{a}\right)^2\right] + A\left[1 - \frac{I_0(\kappa r)}{I_0(\kappa a)}\right]} \tag{23}$$

where $B = a^2 P_z/4\mu$. Differentiating this expression with respect to r yields

$$dt = \frac{L\left[\frac{2Br}{a^2} + \frac{A\kappa I_1(\kappa r)}{I_0(\kappa a)}\right] dr}{\left\{B\left[1 - \left(\frac{r}{a}\right)^2\right] + A\left[1 - \frac{I_0(\kappa r)}{I_0(\kappa a)}\right]\right\}^2} \tag{24}$$

Substituting eq 24 into eq 20 gives

$$E(t) = \frac{2\pi r}{V_1} \frac{\left\{B\left[1 - \left(\frac{r}{a}\right)^2\right] + A\left[1 - \frac{I_0(\kappa r)}{I_0(\kappa a)}\right]\right\}^3}{L\left[\frac{2Br}{a^2} + \frac{A\kappa I_1(\kappa r)}{I_0(\kappa a)}\right]} \tag{25}$$

The volumetric flow rate V_1 can be expressed as

$$V_1 = AA_c\left[1 - \frac{2I_1(\kappa a)}{(\kappa a) I_0(\kappa a)}\right] + \frac{\pi a^2 B}{2} \tag{26}$$

Limiting Cases

If the double layer is very thick, $\kappa a \ll 1$, then eq 17 reduces to

$$U(r) = -\frac{\epsilon\psi_s E_z}{4\mu}(\kappa a)^2\left[1 - \left(\frac{r}{a}\right)^2\right] \tag{27}$$

This is similar to the laminar flow for the case of a pressure-driven flow field; the velocity distribution is parabolic, with a local maximum $U_{max} = -(\epsilon\psi_s E_z/4\mu)(\kappa a)^2$ at the center of the channel. On the other hand, if the double layer is very thin, $\kappa a \gg 1$, then eq 17 gives

$$U(r) = -\frac{\epsilon\psi_s E_z}{\mu} \tag{28}$$

That is, U is independent of r, which is similar to the plug flow in a conventional macrochannel.

If the double layer is very thick, the behavior of the present electroosmotic flow is similar to that of a laminar flow in a cylindrical channel; the minimum residence time $t_{min} = L/U_{max}$ occurs at the center of the microreactor, and the maximum fluid velocity U_{max} is twice the mean fluid velocity U_{avg}, which implies that the mean residence time $t_{avg} = L/U_{avg}$ is twice the minimum residence time. With reference to the residence time distribution (RTD) of a laminar flow in a cylindrical channel, it can be inferred that

$$E(t) = 0, \quad t < t_{min} \tag{29}$$

$$E(t) = \frac{t_{avg}^2}{2t^3}, \quad t > t_{min} \tag{30}$$

If the thickness of the double layer approaches infinity, the velocity distribution arising from the electroosmotic flow approaches a plug flow, and the corresponding RTD is

$$E(t) = \delta(t - t_{avg}) \tag{31}$$

where δ is the Dirac δ function.

Results and Discussion

The governing equations and the associated boundary conditions are solved numerically by Compaq *Visual Fortran* version 6.5 and a Newton−Raphson scheme. For simplicity, possible end effects are neglected. In the numerical simulations, κa, E_z, and P_z are in the ranges [0.001, 500], [2.56×10^5 V/m, 2.56×10^6 V/m], and [0 N/m^3, 10^3 N/m^3], respectively. Other parameters are $a = 10^{-7}$ m, $T = 298$ K, $N_0 = 6.022\,169 \times 10^{23}$ no/mol, $F = 96\,487$ C, $\epsilon = 7.08 \times 10^{-10}$ C/(V·m), and $\mu = 1 \times 10^{-3}$ kg/(ms).

The variations of velocity distribution $U(R)$ at various κa's are shown in Figure 2, and the corresponding variations in residence time distribution $E(t)$ are presented in Figure 3. Figure 2 reveals that the larger the value of κa (the thinner the double layer or the higher the concentration of electrolyte) the faster the fluid velocity is. This is because the higher the concentration of electrolyte the greater the driving force for electroosmotic flow. Three regimes of κa are considered: $\kappa a \ll 1$, $1 < \kappa a < 10$, and $\kappa a \gg 1$. In Figure 2a, $\kappa a \ll 1$, that is, the double layer is thick. In this case, the microreactor is filled with the double layer, and $U(R)$ is close to a parabolic curve. Figure 2b reveals that, if $1 \le \kappa a \le 10$, $U(R)$ starts to deviate from a parabolic curve as κa increases. It becomes flat near the center of the microreactor and drops rapidly near its wall. This is because as the thickness of the double layer decreases the region of the flow field influenced by the charged microreactor declines accordingly. If κa is sufficiently large (>500), the velocity distribution becomes uniform, as can be seen in Figure 2c. The velocity distribution for $\kappa a \ll 1$ is close to a parabolic curve, that is, the corresponding flow field is close to a laminar flow. In this case, $E(t) = t_{avg}^2/2t^3$, according to eq 30, that is, $E(t)$ is inversely proportional to t^3, and there exists a minimum

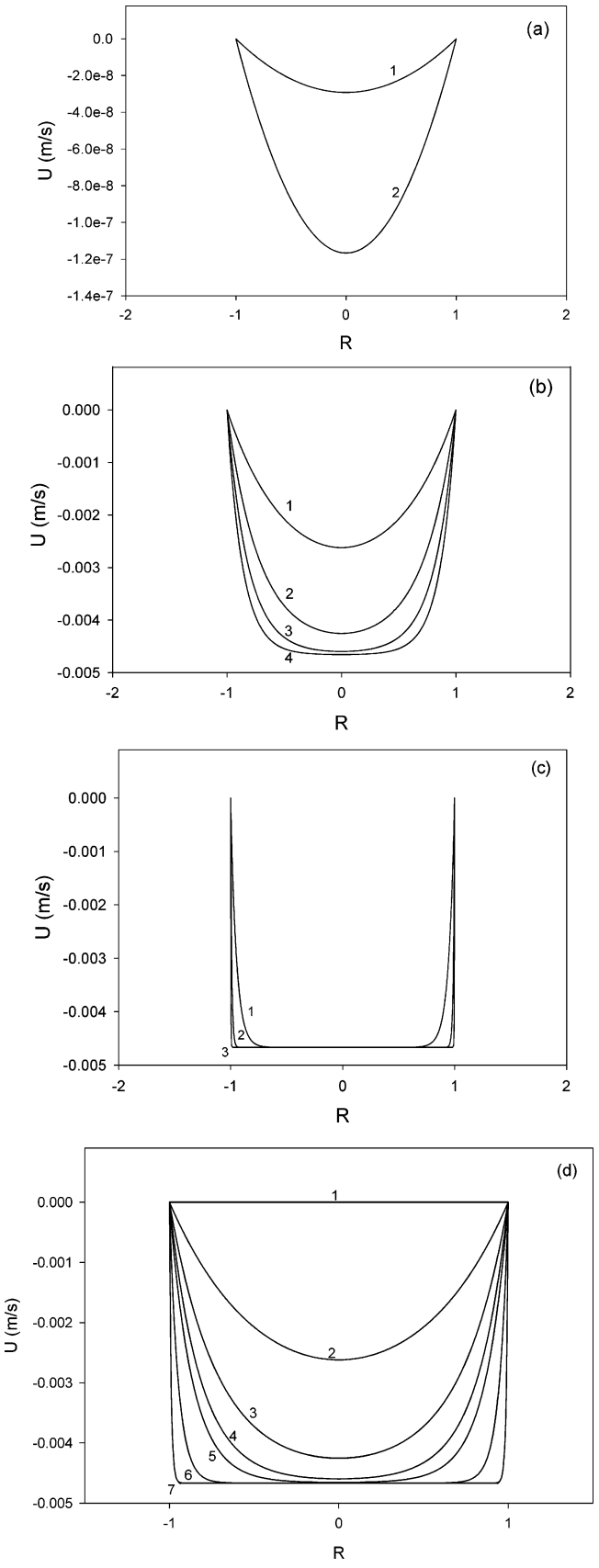

Figure 2. Variation of fluid velocity $U(R)$ at various values of κa for the case when $E_z = 2.56 \times 10^5$ V/m, $P_z = 0$ N/m^3, and $\psi_s = 25.6$ mV. (a) Curve 1, $\kappa a = 0.001$; 2, $\kappa a = 0.005$. (b) Curve 1, $\kappa a = 2$; 2, $\kappa a = 4$; 3, $\kappa a = 6$; 4, $\kappa a = 8$. (c) Curve 1, $\kappa a = 20$; 2, $\kappa a = 100$; 3, $\kappa a = 500$. (d) Curve 1, $\kappa a = 0.001$; 2, $\kappa a = 2$; 3, $\kappa a = 4$; 4, $\kappa a = 6$; 5, $\kappa a = 8$; 6, $\kappa a = 20$; 7, $\kappa a = 100$.

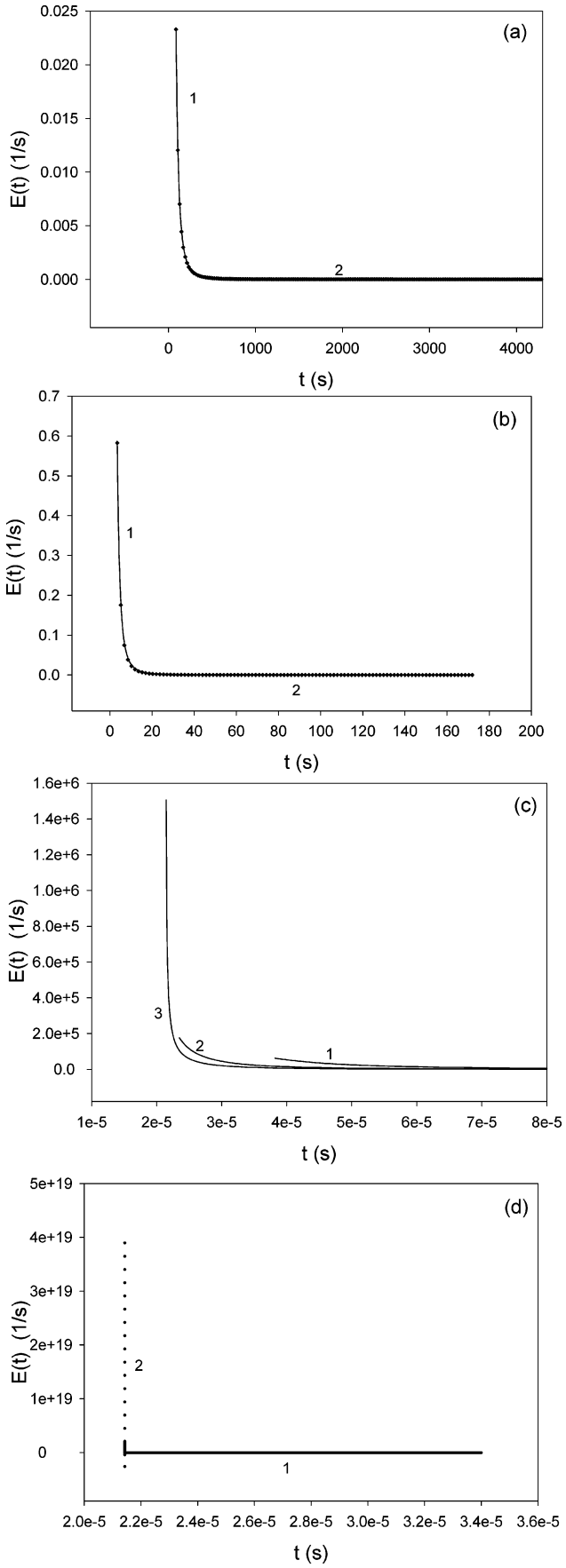

Figure 3. Variation of residence time distribution $E(t)$ for the case when $E_z = 2.56 \times 10^5$ V/m, $P_z = 0$ N/m^3, and $\psi_s = 25.6$ mV. (a) $\kappa a = 0.001$: curve 1, numerical solution; 2, analytical solution. (b) $\kappa a = 0.005$: curve 1, numerical solution; 2, analytical solution. (c) Curve 1, $\kappa a = 2$; 2, $\kappa a = 4$; 3, $\kappa a = 8$. (d) Curve 1, $\kappa a = 100$; 2, $\kappa a = 500$.

TABLE 1: Percentage Deviations of the Minimum Residence Time t_{min} and the Maximum Value of $E(t)$ Based on the Present Numerical Solution from Those Based on the Analytical Solution at Various κa's for the Case When ψ_s = 25.6 mV, P_z = 0 N/m^3, and $E_z = 2.56 \times 10^5$ V/m

	$\kappa a = 0.001$	$\kappa a = 0.005$	$\kappa a = 0.01$
t_{min} (s), numerical solution	85.7240	3.4300	0.8575
t_{min} (s), analytical solution	85.7153	3.4286	0.8571
percentage deviation (%)	0.010	0.041	0.047
maximum value of $E(t)$ (1/s), numerical solution	0.0233	0.5831	2.3326
maximum value of $E(t)$ (1/s), analytical solution	0.0233	0.5826	2.3305
percentage deviation (%)		0.080	0.090

residence time, t_{min}, which occurs at the center of the microreactor and can be expressed as

$$t_{min} = \frac{L}{U_{max}} = \frac{L}{(-\epsilon\psi_s E_z(\kappa a)^2/4\mu)} \tag{32}$$

Figure 3a,b illustrates the $E(t)$ for the case when κa is small (thick double layer), and the minimum residence time and the maximum value of $E(t)$ for the case when κa is small are shown in Table 1; both the results based on the analytical solutions, eqs 29 and 30, and those based on the present numerical solutions are presented. Figure 3a,b and Table 1 reveal that the performance of the present numerical approach is satisfactory. Also, a double layer with scaled thickness $\kappa a = 0.001$ can be considered as infinitely thin. The behavior of $E(t)$ shown in Figure 3c for the case when $1 < \kappa a < 10$ can be explained by referring to the variation of $U(R)$ illustrated in Figure 2b where the larger the κa the faster the electroosmotic flow and the shorter the residence time is. In this case, the portion of fluid that has the minimum residence time becomes larger, because the fluid near the center of the microreactor has the fastest electroosmotic velocity and $U(R)$ is flat in that region. Away from the center of the microreactor, $U(R)$ declines rapidly, and the portion of fluid which has a residence time longer than the minimum residence time is small. Note that the range of $E(t)$ extends to infinity because the velocity on the wall is zero. On the other hand, the smaller the κa is, the slower the electroosmotic velocity, the more uniform the velocity distribution, and the narrower the residence time distribution. Figure 3d shows the influence of κa on $E(t)$ for the case when $\kappa a \gg 1$. As can be seen, if $\kappa a \gg 1$, $U(R)$ approaches a uniform distribution, which is close to a plug flow, and $E(t)$ is close to a Dirac δ function. If $\kappa a \gg 1$, it can be shown that the mean or averaged residence time t_{avg} is $t_{avg} = L/U = L/(-\epsilon\zeta_s E_z/\mu) = 2.142\,88 \times 10^{-5}$ s. Our numerical calculations indicate that $E(t)$ for $\kappa a = 500$ is concentrated at 2.1429×10^{-5} s, but $E(t)$ for $\kappa a = 100$ is relatively widely spread. Therefore, we conclude that a double layer with a scaled thickness $\kappa a = 500$ can be treated as infinitely thin. This is also justified by Table 2, where $E(t)$ for the case when $\kappa a = 500$ is sufficiently close to a Dirac δ function.

The variations of $E(t)$ at various combinations of the scaled applied electric field $E^* = E_z/(RT/FL)$ and κa are illustrated in Figure 4. In general, for a fixed double-layer thickness, the stronger the applied electric field is, the greater the driving force for the electroosmotic flow and the shorter the residence time. Figure 4a shows that the larger E^* is, the narrower the $E(t)$, the larger its maximum, and the greater its range. In Figure 4b, the double layer is thin and the corresponding $E(t)$ value is close to a Dirac δ function. The influence of E^* on $E(t)$ is similar to that in Figure 4a. A comparison between Figures 3 and 4 reveals

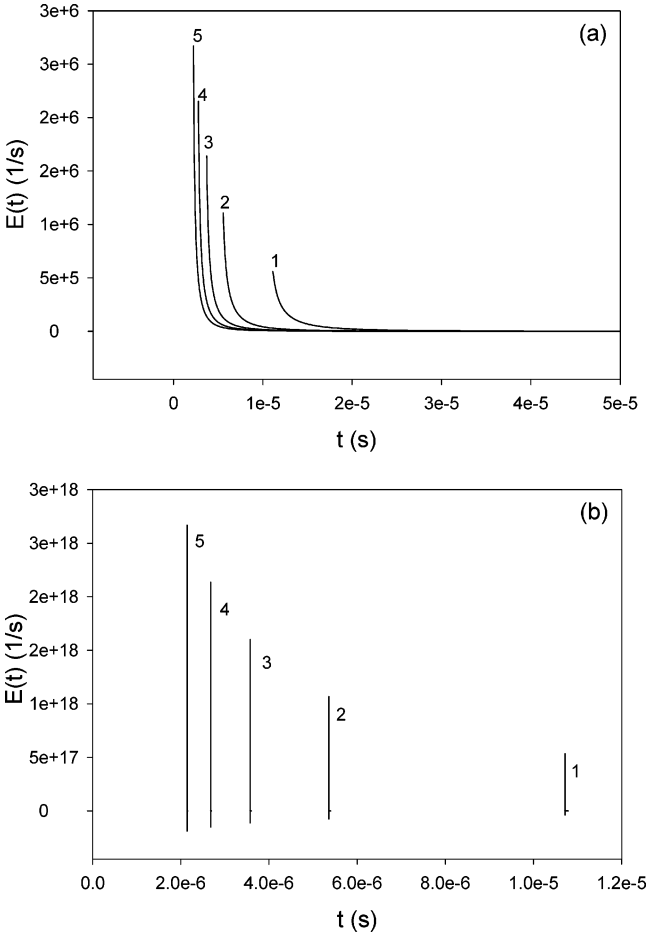

Figure 4. Variation of residence time distribution $E(t)$ at various scaled applied electric field E^* values for different κa's for the case when ψ_s = 25.6 mV and P_z = 0 N/m^3. (a) $\kappa a = 5$; (b) $\kappa a = 500$. Curve 1, $E^* = 2$; 2, $E^* = 4$; 3, $E^* = 6$; 4, $E^* = 8$; 5, $E^* = 10$.

TABLE 2: Maximum of Residence Time Distribution (RTD), Minimum Residence Time, Maximum Residence Time, and Range of Residence Time at Various κa's for the Case When ψ_s = 25.6 mV, P_z = 0 N/m^3, and $E_z = 2.56 \times 10^5$ V/m

	$\kappa a = 20$	$\kappa a = 100$	$\kappa a = 500$
maximum of RTD (1/s)	$2.1410 \times 10^{+10}$	$2.1171 \times 10^{+18}$	$3.8969 \times 10^{+19}$
minimum residence time (s)	2.1429×10^{-5}	2.1429×10^{-5}	2.1429×10^{-5}
maximum residence time (s)	1.2101×10^{-4}	3.4000×10^{-5}	2.1430×10^{-5}
range of residence time (s)	9.9583×10^{-5}	1.2571×10^{-5}	1.0000×10^{-9}

that, when κa (or thickness of the double layer) varies, both the shape and the magnitude of the velocity distribution vary, and therefore, not only the minimum of $E(t)$ but also its shape varies. On the other hand, while the magnitude of the velocity is influenced by E^*, the shape of the velocity distribution remains the same, and therefore, only the residence time and the value of $E(t)$ are influenced by E^*, but the shape of $E(t)$ is the same.

The influences of the applied pressure gradient P_z on the velocity distribution $U(R)$ and on the corresponding $E(t)$ are shown in Figure 5. Here, because the surface potential, the ionic concentration, and the applied electric field are fixed, so is the electrical driving force, and therefore, P_z is the only driving force for fluid flow. As suggested by Figure 2a, if $\kappa a = 0.001$, the velocity distribution is parabolic, and the greater the driving

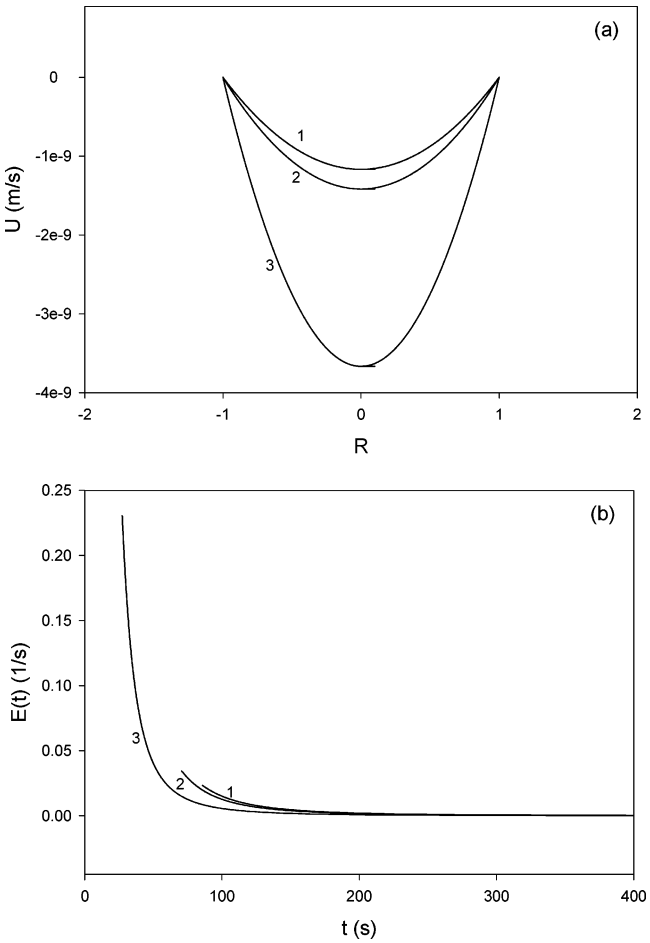

Figure 5. Variation of fluid velocity $U(R)$, (a), and the corresponding residence time distribution $E(t)$, (b), at various applied pressure gradients P_z's for the case when $E_z = 2.56 \times 10^5$ V/m, $\kappa a = 0.001$, and $\psi_s = 25.6$ mV. Curve 1, $P_z = 0$ N/m^3; 2, $P_z = 10^2$ N/m^3; 3, $P_z = 10^3$ N/m^3.

force is, the faster the flow of fluid. Figure 5b indicates that the larger P_z is, the smaller the minimum residence time and the larger the maximum of $E(t)$ and its range: these are expected. The shape of the RTD remains similar, however, because the velocity distribution remains roughly parabolic as P_z varies.

Conclusions

In summary, the residence time distribution (RTD) of a cylindrical microreactor is derived; the results obtained provide necessary information for reactor design and optimization. Under typical conditions, the results of the numerical simulation reveal the following: (a) The thinner the double layer or the higher the concentration of electrolyte, the faster the fluid velocity and the shorter the residence time is. (b) If the double layer is thick, the velocity distribution is close to a parabolic curve, and as its thickness declines, the velocity distribution becomes flat near the center of a microreactor and drops rapidly near its wall. If the double layer is sufficiently thin, the velocity distribution becomes uniform. A double layer thinner than $^1/_{500}$ of the microreactor radius can be considered as infinitely thin, and if it is thicker than 1000× the microreactor radius, then it can be considered as infinitely thick. (c) If the double layer is thick, the RTD is inversely proportional to the cubic power in time, and there exists a minimum residence time, which occurs at the center of a microreactor. (d) In general, the stronger the applied electric field is, the narrower the RTD, the larger its maximum, and the greater its range. (e) When the thickness of the double layer varies, both the shape and the magnitude of the velocity distribution vary, and therefore, not only the minimum of the RTD but also its shape varies. On the other hand, while the magnitude of velocity is influenced by the strength of the applied electric field, the shape of the velocity distribution remains the same, and therefore, only the residence time and the value of the RTD are influenced by the strength of the applied electric field, but its shape remains the same. (f) The influence of the applied pressure gradient is similar to that of the applied electric field.

Acknowledgment. This work is supported by the Department of Economics of the Republic of China under grant 92-EC-17-A-09-S1-019 and the National Science Council of the Republic of China.

References and Notes

(1) Wise, K. D. *Proc. IEEE* **1998**, *86*, 1531−1533.

(2) Löwe, H.; Ehrfeld, W. *Electrochim. Acta* **1999**, *21*−*22*, 3679−3689.

(3) Jensen, K. F. Solid-State Sensor and Actuator Workshop; June 4−8, 2000; pp 105−110.

(4) Manz, A.; Becker, H. *Microsystem Technology in Chemistry and Life Science*; Springer-Verlag: New York, 1998.

(5) Srinivasan, R.; Hsing, I. M.; Berger, P. E.; Firebaugh, S.; Jensen, K. F.; Schmidt, M. A. *AIChE J.* **1997**, *43*, 3059−3069.

(6) Abraham, M.; Ehrfeld, W.; Hessel, V.; Kämper, K. P.; Lacher, M.; Picard, A. *Microelectron. Eng.* **1998**, *41*/*42*, 47−52.

(7) Hsing, I. M.; Srinivasan, R.; Harold, M. P.; Jensen, K. F.; Schmidt, M. A. *Chem. Eng. Sci.* **2000**, *55*, 3−13.

(8) Jensen, K. F. *Chem. Eng. Sci.* **2001**, *56*, 293−303.

(9) Watts, P.; Haswell, S. J.; Pombo-Villar, E. *Chem. Eng. J.* **2004**, *101*, 237−240.

(10) Veser, G. *Chem. Eng. Sci.* **2001**, *56*, 1265−1273.

(11) Rebrov, E. V.; de Croon, M. H. J. M.; Schouten, J. C. *Chem. Eng. J.* **2002**, *90*, 61−76.

(12) Claus, P.; Hönicke, D.; Zech, T. *Catal. Today* **2001**, *67*, 319−339.

(13) Burgreen, D.; Nakache, F. R. *J. Phys. Chem.* **1964**, *68*, 1084−1091.

(14) Rice, C. L.; Whitehead, R. *J. Phys. Chem.* **1966**, *69*, 4017−4024.

(15) Sørensen, T. S.; Koefoed, J. *J. Chem. Soc., Faraday Trans.* **1974**, *70*, 665−675.

(16) Jacobson, S. C.; Mcknight, T. E.; Ramsey, J. M. *Anal. Chem.* **1999**, *71*, 4455−4459.

(17) Ermakov, S. V.; Jacobson, S. C.; Ramsey, J. M. *Anal. Chem.* **1998**, *70*, 4494−4504.

(18) Patankar, N. A.; Hu, H. H. *Anal. Chem.* **1998**, *70*, 1870−1881.

(19) Jacobson, S. C.; Ramsey, J. M. *Anal. Chem.* **1997**, *69*, 3212−3217.

(20) Barker, S. L. R.; Ross, D.; Tarlov, M. J.; Gaitan, M.; Locascio, L. E. *Anal. Chem.* **2000**, *72*, 5925−5929.

(21) Bianchi, F.; Ferrigno, R.; Girault, H. H. *Anal. Chem.* **2000**, *72*, 1987−1993.

(22) Cummings, E. B.; Griffiths, S. K.; Nilson, R. H.; Paul, P. H. *Anal. Chem.* **2000**, *72*, 2526−2532.

(23) Ermakov, S. V.; Jacobson, S. C.; Ramsey, J. M. *Anal. Chem.* **2000**, *72*, 3512−3517.

(24) Mitchell, M. J.; Qiao, R.; Aluru, N. R. *J. Microelectromech. Syst.* **2000**, *9*, 435−449.

(25) Ajdari, A. *Phys. Rev. E* **2001**, *65*, 016301−1−016301−9.

(26) Ren, L.; Li, D.; Qu, W. *J. Colloid Interface Sci.* **2001**, *233*, 12−22.

(27) MacInnes, J. M. *Chem. Eng. Sci.* **2002**, *57*, 4539−4558.

(28) Takhistov, P.; Duginova, K.; Chang, H. C. *J. Colloid Interface Sci.* **2003**, *263*, 133−143.

(29) Froment, G. F.; Bischoff, K. B. *Chemical Reactor Analysis and Design*; Wiley: New York, 1990.

(30) Fogler, H. S. *Elements of Chemical Reaction Engineering*; Prentice Hall: Upper Saddle River, NJ, 1999.

(31) Levenspiel, O. *Chemical Reaction Engineering*; Wiley: New York, 1999.